"Direct observation" of the atomic structure of a crystal in a high-resolution electron microscope

V. L. Indenbom and S. B. Tochilin

A. V. Shubnikov Institute of Crystallography, Academy of Sciences of the USSR
(Submitted 20 March 1990)
Zh. Eksp. Teor. Fiz. **98**, 1402–1411 (October 1990)

When high-energy electrons are diffracted by a crystalline foil, the channeling of the electrons reveals atomic chains running parallel to the transmission direction. However, the images of light chains oscillate, and those of heavy chains exhibit a steady fading. Moreover, the contrast maxima do not coincide with the coordinates of chains, and various secondary maxima and intensity spikes appear along the borders of two-dimensional (projected) cells, where there are no atoms at all. Distortions like these in the images of the atomic structure of crystals have been seen in previous experiments, but they have erroneously been attributed to imperfections of the electron-optical systems of the microscopes. In reality, diffraction effects rule out any "direct observation" of the atomic structure of a crystal in a high-resolution electron microscope at the present state of the art (at a resolution of 1–2 Å), and they will continue to do so regardless of any future progress in the design of electron microscopes or improvements in their resolution.

Qualitative improvements in electron optics have resulted in the attainment of a resolution of 1–2 Å in advanced electron microscopes, making it possible to reliably observe individual atoms on a structureless substrate.[1] It is a more complicated matter to observe atoms at the surface of a crystal or to observe atomic chains in a crystal, not to mention point defects of the crystal lattice. The fervent desire of experimentalists to directly observe the atomic structure of crystals in an electron microscope frequently leads them to throw caution to the wind in interpreting the observed patterns and to forget about the diffraction properties of the image. Under the conditions prevailing in high-resolution electron microscopy, the electrons diffracted in a crystalline foil under study constitute a complex set of quasiparticles. As in the quantum theory of channeling, a special role is played by a specific class of tightly bound quasiparticles which arise as the crystal is scanned along close-packed atomic chains and which correspond to channeling of electrons along these chains. In this case, deep transverse-motion levels arise in the potential wells formed by the atomic chains. The wave field therefore becomes qualitatively different from that in ordinary transmission electron microscopy. In particular, sharp oscillations in the flux of electrons, both transverse and as a function of depth, appear. We have previously[2] discussed the case, typical of light chains, in which one highly localized $1s$ wave dominates, being channeled strictly along an atomic chain and periodically undergoing diffractive focusing. As a result, the intensity of the electron flux to which the chain is exposed increases by a factor of nearly 50.

In the present paper we take up the general case of normal transmission, in which an entire series of ns Bloch waves ($n = 1, 2, 3, \ldots \infty$) are excited simultaneously. We examine not only the image of atomic chains corresponding to the central peaks of the ns waves but also various "false maxima." In particular, we single out the case in which the central peaks of the ns waves cancel each other out, and the electrons being channeled along the atomic chains form halos around the chains, i.e., "annular" images of these chains, while the chains themselves are unseen. We will show that the necessary condition for this cancellation corresponds to parameter values which are characteristic of the high-resolution electron microscopy of a long list of crystals containing heavy atoms. The extinction of the images of heavy atomic chains, accompanied by the simultaneous appearance of false maxima of various types, is a particularly serious complication in efforts to decipher high-resolution electron micrographs of "mixed" crystals, by which we mean crystals containing both heavy and light atoms.

As a typical example, which clearly illustrates the problem of annular images, we might cite the high-resolution electron micrograph of the atomic structure of gold which was recorded by Hashimoto[3] and which attracted worldwide interest (Fig. 1). Instead of intensity maxima centered on atomic chains on this photograph, which corresponds to a [001] projection, there are clearly defined annular halos, whose nature has heretofore been a matter of guesswork. Hashimoto himself discussed the possibility of using photomicrographs of this type to study the "internal structure of atoms."[4] This image was interpreted by Thomas and Goringe[5] as a phase contrast which made it possible to directly resolve individual atomic chains. Danishevskiĭ and Chukhovskiĭ[6] explained Hashimoto's annular images in terms of electron-optical factors which limit the resolution of an electron microscope: defocusing and the finite dimensions of the aperture diaphragm. It was asserted in Vaĭnshteĭn's review[1] that the extinction of the images of the gold atoms was a consequence of an alternation of the signs of the contrast transfer function of the electron microscope. Spence suggested in a monograph[7] that such images are a consequence of multiple scattering. In the face of all these attempts to guess the nature of the effect, we have asserted[8–10] that the annular images form as a result of interference effects in the wave field which arises in a crystalline foil when high-energy electrons are sent through it. This wave field results from channeling of electrons along the periphery of potential wells. Below we prove this assertion.

As another example we will discuss a micrograph of an Si_3N_4 crystal obtained on a Dutch microscope with a resolution of 2 Å at the Materials Science Center of the Paris

 0038-5646/90/100782-06$03.00

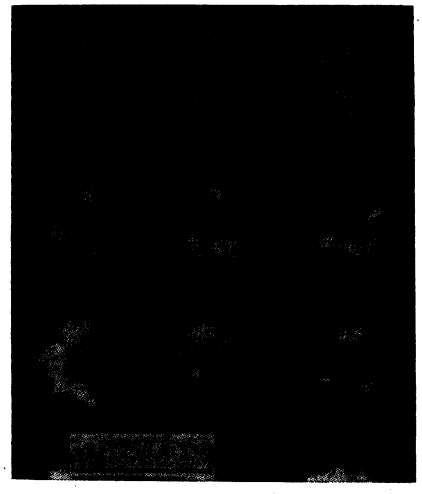

FIG. 1.

School of Mining (Fig. 2). There are some strange intensity spikes between atoms, which the authors declared to be "a glassy phase within the crystalline structure of Si_3N_4."[11] We will demonstrate that this micrograph actually is conveying a completely unexotic intensity peak of a diffractive nature at the boundaries of two-dimensional (projected) unit cells (at the boundaries of Voronoy cells in the general case of a real crystal), where the highly localized fundamental waves make only a minor contribution, where spatial modulations of the wave field are suppressed, and where the electron beam incident on the crystal passes through the crystal essentially unobstructed.

In this manner we will prove that the distortion of the image of the atomic structure of a crystal is completely predictable and is a consequence of interference effects which occur in the wave field which arises in a crystalline foil when high-energy electrons are sent through it. It is not a consequence of the design of the electron microscope. Therefore, no matter how high the resolution, the images of chains of heavy atoms will be intermingled with the images of empty channels, and secondary (false) maxima will be intermingled with the images of light chains or of atoms outside chains oriented parallel to the beam direction.

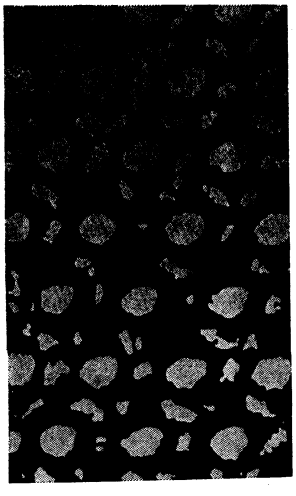

FIG. 2.

1. CONSTRUCTION OF BOUND *ns* BLOCH WAVES

As was shown in Ref. 2, in the construction of tightly bound states the potential of an atomic chain can be described approximately by

$$V(r)=-\frac{Ze^2a_{TF}}{rd}, \tag{1}$$

where Z is the atomic number, e is the electron charge, a_{TF} is the Thomas–Fermi screening radius, and d is the mean distance between atoms in the chain. When the electron beam enters the crystal in the direction along chains oriented perpendicular to the entrance surface, the bound states are *ns* waves which satisfy a two-dimensional Schrödinger equation. After factorization, this equation can be written

$$\frac{\hbar^2}{2m}\frac{1}{r}\frac{\partial}{\partial r}\left[r\frac{\partial}{\partial r}\Phi_{ns}(r)\right]+V(r)\Phi_{ns}(r)=E_{ns}^{\perp}\Phi_{ns}(r),$$

$$E_{ns}^{\perp}=-\frac{\hbar^2}{2m}\frac{1}{\rho^2}\gamma_n^2, \quad n=1,2,\ldots, \tag{2}$$

where $E_{ns}^{\perp}$ is the transverse energy, $\gamma_n=(n-1/2)^{-1}$, and

$$\rho=\frac{\hbar^2 d}{mZe^2a_{TF}} \tag{3}$$

is a length scale which will be used below as the unit of distance. This length scale incorporates the chain density d, the particular nature of the chain (through a_{TF}), the charge Z of the nucleus, and the energy of the incident beam (through the relativistic electron mass m).

From Eq. (2) we find the following result for *ns* waves:

$$\Phi_{ns}(r)=M_n\exp(-\gamma_n r)\sum_{k=0}^{n-1}B_k(\gamma_n r)^k. \tag{4}$$

Here the M_n are normalization coefficients, and the coefficients B_k are given by

$$B_k=\frac{(-2)^k(n-1)!}{(k!)^2(n-k-1)!}. \tag{5}$$

The normalization coefficients M_n must be chosen in such a way that the wave functions are normalized to, for example, unit resultant intensity on the area per atomic chain, S. In other words, for highly localized states we would have

$$2\pi\rho^2\int_0^R\Phi_{ns}(r)\Phi_{ns}^{*}(r)r\,dr=1, \tag{6}$$

where

$$R=(S/\pi\rho^2)^{1/2} \tag{7}$$

is the dimensionless radius corresponding to the area S. For normal incidence of an electron beam with unit amplitude, the excitation coefficients A_{ns} are found from the condition

$$\sum_n A_{ns}\Phi_{ns}(r)=1, \tag{8}$$

from which we in turn find

$$A_{ns}=2\pi\rho^2\int_0^R\Phi_{ns}^{*}(r)r\,dr. \tag{9}$$

In addition to the highly localized *ns* Bloch waves, poorly localized waves with large values of n, which pass

through the foil without a phase disruption, are involved in the expansion (8) (Ref. 8). If the wave functions in (4) are well localized within a unit cell, we can set $R \to \infty$ in (6) and (9). All the integrals then reduce to tabulated integrals (even for finite R). In the case $R = \infty$ the coefficients M_n and A_n can be written in the form

$$M_n = -\frac{\gamma_n}{\rho}\sqrt{\frac{2}{\pi}}\left[\sum_{i,j=0}^{n-1}\sum B_i B_j \frac{(i+j+1)!}{2^{i+j}}\right]^{-1/2}, \qquad (10)$$

$$A_n = 2\pi M_n \left(\frac{\rho}{\nu}\right)^2 \sum_{i=0}^{n-1} B_i (i+1)! \qquad (11)$$

If the distance between chains approaches the length scale of the decay of the wave functions Φ_{ns} constructed on the basis of individual chains, it becomes necessary to consider a two-dimensional lattice of chains instead of isolated chains. In this case we can use the tight-binding approximation (Ref. 12, for example), in which an orbital constructed from the wave functions of isolated chains serves as a seed wave function. A structure factor naturally arises in the summation over chains, while overlap integrals arise in the course of the normalization. As a rule, however, the distances between chains are significantly greater than the length scales for the decay of the first wave functions $\Phi_{ns}(r)$, so the approximation of isolated chains is a good one in problems in which explicit expressions are required for only the first few well-localized Bloch waves.

2. EXTINCTION OF IMAGES OF ATOMIC CHAINS AND APPEARANCE OF ANNULAR IMAGES

Figure 3, a–c, shows the first three Bloch functions for 1*s*, 2*s*, and 3*s* waves in the case of crystals consisting of comparatively heavy atomic chains. In this case the first two functions correspond to levels deep below the barrier and are well localized, while the third corresponds to a level near the barrier and is localized only poorly. This case is typical of, for example, Au [001], W [001], and Nb [110]. If the potential (1) is continued to $d_\perp/2$, where $d_\perp$ is the distance between neighboring chains, the $E_{ns}^{\perp}$ level of the Φ_{ns} wave is a below-barrier level under the condition

$$d_\perp/\rho \geqslant (2n-1)^2. \qquad (12)$$

Using the methods of Refs. 2 and 8 for dealing with Bloch waves collectively in the case in which the two waves Φ_{1s} and Φ_{2s} are below the barrier, while the wave Φ_{3s} is only poorly

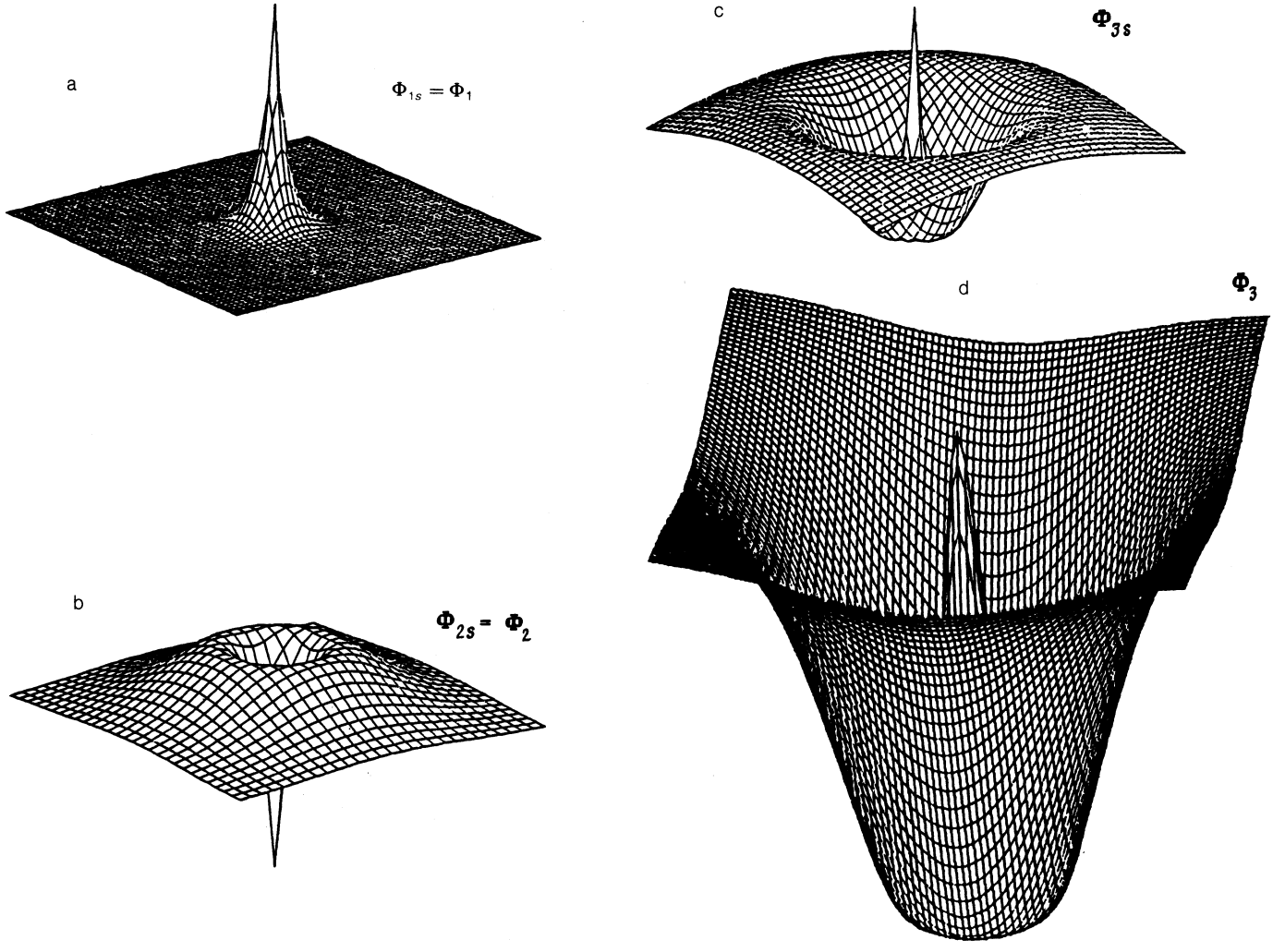

FIG. 3.

localized, we would like to incorporate the wave Φ_{3s} in a general "background." For simplicity below we denote $A_{1s}\Phi_{1s}$ by Φ_1, $A_{2s}\Phi_{2s}$ by Φ_2, and the "background" by Φ_3. From the boundary condition (8) we find the following expression for the background:

$$\Phi_3(r)=1-\Phi_1(r)-\Phi_2(r). \tag{8'}$$

The function $\Phi_3(r)$ is orthogonal with respect to $\Phi_1(r)$ and $\Phi_2(r)$; we have $\Phi_3=0$ at $r=0$; and as the distance from the chain increases and the functions $\Phi_1(r)$ and $\Phi_2(r)$ decay, the function $\Phi_3(r)$ approaches unity (Fig. 3d).

It is not difficult to see that the annular images stem from the ns Bloch waves with $n\geqslant 2$, which have significant excitation coefficients according to (11). The presence of a single strong wave, namely, a $2s$ wave, is not by itself sufficient for the formation of annular images, since this wave has a significant central peak, which would create a corresponding bright central spot (Fig. 2b). In order to extinguish this spot, we need to arrange the mutual cancellation of the contributions of the central peaks of all ns waves. Using the method of Refs. 2 and 8, we can rigorously calculate the conditions for the extinction of the "regular" image of the atomic structure and for the appearance of bright halo rings around the atomic chains.

In general, the intensity at the exit surface of the foil, $z=t$, can be written as follows, where we are using the boundary condition (8) at $z=0$ and making use of the reality of the functions Φ_i:

$$I(r,t)=1+2\sum_{i>j}\Phi_i(r)\Phi_j(r)\left\{\cos\left[2\pi\left(\frac{1}{L_i}-\frac{1}{L_j}\right)t\right]-1\right\}, \tag{13}$$

where L_i is the oscillation period of the Bloch wave Φ_i into the crystal. When the three waves $\Phi_1(r)$, $\Phi_2(r)$, $\Phi_3(r)$ are excited in the crystal, it is convenient to construct images at characteristic depths z_i $(i=1,2,3)$ given by

$$z_i=|L_n^{-1}-L_m^{-1}|^{-1} \qquad (n,\ m\neq i,\ n>m). \tag{14}$$

These characteristic depths correspond to matching of the phases of the waves Φ_n and Φ_m. At the depths in (14) the wave field can be expressed in terms of the amplitude of only one of the waves, namely, the amplitude of the wave Φ_i at the depth z_i. The field intensity of this depth can be written in the form

$$I(r,\ z_i)=1+I_i(r)\,T(z_i), \tag{15}$$

where

$$I_i(r)=\Phi_i(r)\,[\Phi_i(r)-1], \tag{16}$$

$$T(z_i)=2\{\cos[2\pi(L_n^{-1}-L_i^{-1})z_i]-1\}$$

$$=2\{\cos[2\pi(L_m^{-1}-L_i^{-1})z_i]-1\}. \tag{17}$$

Using (13), we can show that the intensity at an arbitrary depth can be written as a superposition of the characteristic intensities in (16). To demonstrate this point, we write each term of the sum (13) in the form

$$2\Phi_i(r)\Phi_j(r)=I_n(r)-I_i(r)-I_j(r), \qquad i\neq n\neq j, \tag{18}$$

and we rewrite (13) in the form

$$I(r,t)=1+\sum_i I_i(r)P_i(t), \tag{19}$$

where

$$P_i(t)=1+\cos[2\pi(L_n^{-1}-L_m^{-1})t]$$
$$-\cos[2\pi(L_n^{-1}-L_i^{-1})t]-\cos[2\pi(L_m^{-1}-L_i^{-1})t]. \tag{20}$$

A necessary and sufficient condition for the central peaks of the $1s$ and $2s$ waves to be in phase and to cause a maximum reduction of the resultant contribution to the intensity of the central peak, is that, in accordance with (14), the crystal thickness be a multiple of the characteristic depth

$$z_3=[(L_{1s})^{-1}-(L_{2s})^{-1}]^{-1}. \tag{21}$$

Using the relation between the length L_{ns} and the level $E_{ns}^{\perp}$ given in Ref. 8,

$$L_{ns}=2\lambda E/E_{ns}^{\perp}, \tag{22}$$

where λ and E are the wavelength and energy of the incident electron beam, and substituting the values of $E_{1s}^{\perp}$ and $E_{2s}^{\perp}$ from expression (2), we finally find

$$z_3=(3/2\pi)^2\rho^2/\lambda, \tag{23}$$

where ρ is the characteristic length (3). Substituting in numerical parameter values for a [001] gold foil on which a beam of 100-keV electrons is incident normally, we reach the conclusion that the oscillations associated with the interference of the waves Φ_{1s} and Φ_{2s} corresponds to an extinction length $t=30$ Å. These oscillations periodically reduce the intensity of the central peak to a level corresponding roughly to the level of the beam incident on the foil. Between these dips, the intensity at the top of the central peak is increased by a factor of tens. However, the width of this peak is much smaller than the resolution of ordinary microscopes, so its image is blurred, and its intensity turns out to be lower than that of the surrounding halo. Characteristic annular images of the chains arise.

With increasing depth in the foil, the ns waves with $n>2$ make a progressively increasing contribution to the image. Assuming thicknesses which are multiples of z_3 $(t=Nz_3, N=1,2,...)$; assuming the conditions $L_3\gg L_2, L_1$; and using (2) and (22), from which we find $L_1/L_2=1/9$, we can write the intensity (15)–(17) in the form

$$I(r,\ t)=1+2I_3(r)\,[1-\cos(\pi N/4)]. \tag{24}$$

With $N=4$, i.e., with $t=120$ Å, and also with $N=12$, 20, 28,..., the image intensity becomes $I(r)=1+4I_3(r)$, and the ring intensity reaches a maximum according to (16) and (8'). The image of the chains, on the other hand, is essentially extinguished, since what is left at the center is a very narrow peak of unit height, formed by the sum $\Phi_1+\Phi_2$. This peak has been shrunk by a factor of several units because of electron-optics factors of the microscope, since the width of this peak is much smaller than the resolution [see Fig. 4, which shows cross sections of $I(r,t)$ for various thicknesses of the crystalline foil]. According to (24), the oscillation period of the annular images is $8z_3=240$ Å, so the extinction of the chains is an extremely stable effect as a function of depth.

The variation in the resultant wave field, (13), as a function of depth in the foil can be described by means of phase diagrams in a complex plane. For each Bloch wave

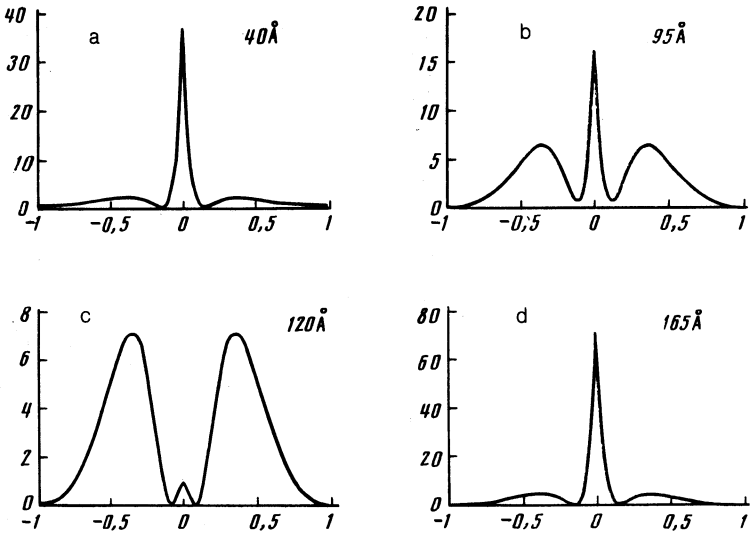

FIG. 4.

$B_m\Phi_m(\mathbf{r})\exp(ik_m z)$ the excitation coefficient B_m determines the length of the radius vector, $B_m\Phi_m(\mathbf{r})$, while the phase $\mathrm{Im}(B_m\Phi_m) + k_m z$ specifies the angle through which this vector is rotated with respect to the abscissa. The term $k_m z$ corresponds to a uniform rotation of the radius vector with increasing z, so the overall picture is reminiscent of the solar system (Fig. 5). For each point $\mathbf{r}$ in real space, the sum in (12) corresponds to a sum of the radius vectors of Bloch waves.

Figure 6 illustrates the image intensity at the exit surface of the foil, (13), under conditions (Au [001], 100 keV, $t = 120$ Å) such that the foil thickness reaches an optimum foil for the observation of the annular images. It does not follow, however, that the annular images in the experiments of Ref. 3 were obtained simply by chance. According to the discussion above, these images are completely characteristic of chains of heavy atoms when the wave Φ_{3s} is a near-barrier wave. They appear over a wide range of typical foil thicknesses according to (19), (20), and (24). One can also see that the annular images could not arise from (and could not be greatly spoiled by) structural imperfections of the microscope. At a resolution of 1–2 Å, the halos around the chains are not spoiled, while the sharp central peaks are simply blurred and rendered invisible.

3. IMAGE OF THE BOUNDARIES OF UNIT CELLS

It clearly follows from the boundary condition (8) that the resultant amplitude of the Bloch waves with $n \gg 1$ must be very large near the boundaries of two-dimensional unit cells constructed for a structure projected along the axis of the incident beam. The reason is that the amplitude of the highly localized Bloch waves, which channel along atomic chains, is small there. Adding together, these waves form a common "background" wave, which passes through the foil without phase disruption.[8] As a result, the wave field at the exit surface of the foil retains the amplitude which prevailed at the entrance surface (we are ignoring absorption) near the boundaries of unit cells (more precisely, near the boundaries of two-dimensional Voronoy cells, since a real crystal could not have a single unit cell!). This effect could be observed on the image of any sample if the bright images of the atomic chains were suppressed by varying either the diffraction conditions or the intensity detection conditions.

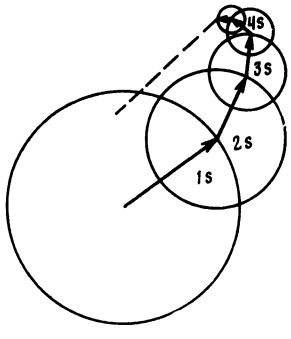

FIG. 5.

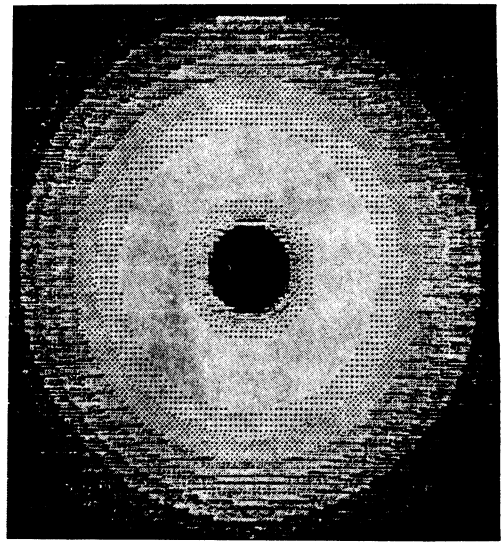

FIG. 6.

The photograph in Fig. 2 is a good illustration of these assertions. Intensity peaks appear on the image where there are no atoms at all. Particularly obvious are the vertices of the unit-cell boundaries which lie farthest from the atomic chains on which the localized Bloch waves are centered. Using the tight-binding method, we can estimate the width of the boundary regions which are imaged with unit intensity (if there is no absorption). For the case discussed above, Au [001], the effect can be illustrated by Fig. 3d, where the image amplitude at the edges of the two-dimensional unit cell is comparable in magnitude to the amplitude of the central peak. Since this peak is narrow, one can assert that electron-optics factors will reduce the intensity of the central peak and that the boundaries of the unit cells will emerge clearly superposed on the weak central peak surrounded by a halo.

If a crystal contains both heavy and light chains, "direct observation" of its atomic structure is impossible, regardless of any future progress in the resolution of microscopes: Because of the superposition of Bloch waves corresponding to different periods L_i, the images of light and heavy chains will oscillate with different extinction lengths. The heavy chains will be completely extinguished and will appear as empty channels. The halos around heavy chains will be superimposed on each other and will create false maxima which flicker along depth. Secondary (but stable) maxima will also appear at the boundaries of Voronoy zones. This entire complex diffraction pattern absolutely cannot be regarded as constituting a "direct observation" of the atomic structure of a crystal lattice, and it cannot be interpreted directly, without auxiliary experiments and without the use of the quantum theory of the diffractive image of a crystal lattice.

[1] B. K. Vaĭnshteĭn, Usp. Fiz. Nauk **152**, 75 (1987) [Sov. Phys. Usp. **30**, 393 (1987)].
[2] V. L. Indenbom and S. B. Tochilin, Kristallografiya **32**, 586 (1987) [Sov. Phys. Crystallogr. **32**, 341 (1987)].
[3] H. Hashimoto, H. Endoh, T. Tanji *et al.*, J. Phys. Soc. Jpn. **42**, 1073 (1977).
[4] H. Hashimoto, Y. Yokota, H. Endoh, and A. Kumao, Chem. Scr. **14**, 125 (1978).
[5] G. Thomas and M. J. Goringe, *Transmission Electron Microscopy of Materials*, Wiley-Interscience, New York, 1979 (Russ. Transl. Nauka, Moscow, 1983).
[6] A. L. Danishevskiĭ and F. N. Chukhovskiĭ, Kristallografiya **27**, 668 (1982) [Sov. Phys. Crystallogr. **27**, 401 (1982)].
[7] J. Spence, *Experimental High-Resolution Electron Microscopy*, Oxford Univ. Press, London, 1981 (Russ. Transl. Nauka, Moscow, 1986).
[8] V. L. Indenbom and S. B. Tochilin, Kristallografiya **32**, 1353 (1987) [Sov. Phys. Crystallogr. **32**, 795 (1987)].
[9] V. L. Indenbom and S. B. Tochilin, in Proceedings of the Twelfth European Cryst. Meeting, Vol. 1, 20–29 August 1989, p. 32.
[10] V. L. Indenbom and S. B. Tochilin, Dokl. Akad. Nauk SSSR 1990.
[11] "Industries et technique," 1986, No. 577, Nauka i zhizn', No. 8, p. 48.
[12] N. W. Ashcroft and N. D. Mermin, *Solid State Physics*, Holt, Rinehart & Winston, Inc., New York, N.Y., 1976 (Russ. Transl. Mir, Moscow, 1979).

Translated by D. Parsons